Design, Fabrication, and Assembly of the SPARC Toroidal Field Model Coil

Rui F. Vieira, David Arsenault, Raheem Barnett, Larry Bartoszek, William Beck, Sarah Chamberlain, J. L. Cheng, Eric Dombrowski, Jeffrey Doody, Darby Dunn, Jose Estrada, Vincent Fry, Sarah Garberg, Theodore Golfinopoulos, Aliya Greenberg, Samuel Heller, Amanda Hubbard, Daniel Korsun, Sergey Kuznetsov, Brian LaBombard, Chris Lammi, Rick Leccacorvi, Matthew Levine, David Chavarria Mendoza, Kristen Metcalfe, Philip Michael, Theodore Mouratidis, Robert Mumgaard, J. P. Muncks, Richard Murray, Daniel Nash, Andrew Pfeiffer, Samuel Pierson, Alexi Radovinsky, Ron Rosati, Michael Rowell, Erica Salazar, Shane Schweiger, Syun'ichi Shiraiwa, Brandon Sorbom, Peter Stahle, Ken Stevens, Deepthi Tammana, Thomas Toland, Matthew Vernacchia, Erik Voirin, Alex Warner, Amy Watterson, Dennis G. Whyte, Sidney Wilcox, Lihua Zhou, Alexander Zhukovsky, and Zachary S. Hartwig

***Abstract*—The SPARC Toroidal Field Model Coil (TFMC) is the first large-scale (∼3 m), high-field (∼20 T) superconducting fusion magnet based on Rare Earth Yttrium Barium Copper Oxide (REBCO). Weighing 10,058 kg and utilizing 270 km of REBCO, the TFMC is a non-insulated, stack-in-plate style superconducting magnet. It has three main components: (1) the winding pack; (2) the structural case; and (3) the case extensions, or plena. The winding pack is composed of sixteen single pancakes with two termination plates top and bottom. The pancakes are Nitronic 40 radial plates machined with spiral channels on one side for the REBCO tape stack and single-pass channels on the opposite side for supercritical helium coolant. After assembly, each pancake undergoes a vacuum-pressure impregnation solder process to provide good mechanical protection of the REBCO tape stack and efficient thermal and electrical connectivity within each pancake. The pancakes are bolted along the inner and outer perimeter to provide mechanical and thermal connectivity while inter-pancake joints provide low resistance current transfer between pancakes. The top and bottom termination plates facilitate electrical connection to a superconducting feeder system. Embedded throughout the winding pack are 211 voltage taps, 34 temperature sensors, 34 helium flow monitors, 4 Hall probes, and 4 resistive surface heaters. The winding pack is contained within a structural case, a "trough and lid" style design composed of two Nitronic 50 forgings machined to shape and bolted together. The case reacts the large electromechanical stresses approaching 1 GPa during operation and serves as a pressure vessel that enables 20 bar supercritical helium flow that cools the winding pack and case. Two case extensions are attached to the case with unique high-pressure feedthroughs to provide winding pack access for current, cooling, and instrumentation, completing the magnet assembly.**

***Index Terms*—Fusion energy, high-temperature superconductor, SPARC, superconducting magnet, toroidal field model coil (TFMC).**

I. Introduction

THE SPARC Toroidal Field Model Coil (TFMC) Project was an approximately three-year effort between 2018 and 2021 that developed novel rare earth yttrium barium copper oxide (REBCO) superconductor technologies [1], [2], [3], [4] and then utilized those technologies to successfully design, build, and test a first-in-class high-field (∼20 T) representative scale (∼3 m) superconducting toroidal field (TF) coil. With the principal objective of retiring the design, fabrication, and operational risks inherent in large-scale no-insulation (NI) REBCO superconducting magnets for fusion energy devices, the project was executed jointly by the MIT Plasma Science and Fusion Center (PSFC) and Commonwealth Fusion Systems (CFS) as a critical technology enabler of the high-field pathway to fusion energy [5] and, in particular, as a risk retirement program for the TF magnet in the SPARC tokamak [6].

This article is part of a collection of papers [7], [8], [9], [10], [11] intended to cover the principal parts of the TFMC project, including the design and fabrication of the magnet, the design and assembly of the test facility, and an overview of the results from the experimental test campaigns carried out in the Fall of 2021. The focus of this article is on the TFMC itself, shown as a completed assembly in Fig. 1. The TFMC represents a step change in superconducting magnet technology. Relative to previous large-scale fusion superconducting magnets, such as

Manuscript received 24 August 2023; revised 4 December 2023; accepted 10 January 2024. Date of publication 22 January 2024; date of current version 19 February 2024. This work was supported by Commonwealth Fusion Systems (CFS). *(Corresponding author: Rui F. Vieira.)*

Rui F. Vieira, David Arsenault, William Beck, Jeffrey Doody, Jose Estrada, Vincent Fry, Theodore Golfinopoulos, Amanda Hubbard, Daniel Korsun, Brian LaBombard, Rick Leccacorvi, Philip Michael, Theodore Mouratidis, Richard Murray, Andrew Pfeiffer, Samuel Pierson, Alexi Radovinsky, Ron Rosati, Michael Rowell, Erica Salazar, Shane Schweiger, Syun'ichi Shiraiwa, Peter Stahle, Thomas Toland, Amy Watterson, Dennis G. Whyte, Lihua Zhou, Alexander Zhukovsky, and Zachary S. Hartwig are with MIT Plasma Science and Fusion Center, Cambridge, MA 02139 USA (e-mail: vieira@psfc.mit.edu).

Raheem Barnett, Sarah Chamberlain, J. L. Cheng, Eric Dombrowski, Darby Dunn, Sarah Garberg, Aliya Greenberg, Samuel Heller, Sergey Kuznetsov, Chris Lammi, Matthew Levine, David Chavarria Mendoza, Kristen Metcalfe, Robert Mumgaard, J. P. Muncks, Daniel Nash, Brandon Sorbom, Ken Stevens, Deepthi Tammana, Matthew Vernacchia, Alex Warner, and Sidney Wilcox are with Commonwealth Fusion Systems, Devens, MA 01434 USA.

Larry Bartoszek is with Bartoszek Engineering, Aurora, IL 60506 USA.

Erik Voirin is with eVoirin Engineering Consulting, Batavia, IL 60510 USA.

Color versions of one or more figures in this article are available at https://doi.org/10.1109/TASC.2024.3356571.

Digital Object Identifier 10.1109/TASC.2024.3356571

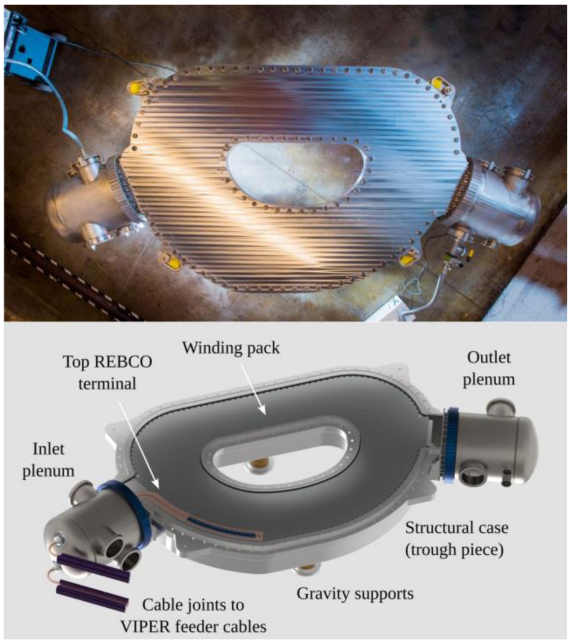

Fig. 1. Top-down view of the completed TFMC ready for initial experimental testing (top) accompanied by a CAD rendering highlighting key features of the magnet (bottom).

TABLE I
COMPARISON OF THE KEY PARAMETERS FOR THE TFMC AND ONE OF THE 18 COILS THAT FORM THE SPARC TF MAGNET

Design parameter	TFMC	TF coil
Magnet mass [kg]	10 058	18 025
Magnet size [m]	2.9 × 1.9	4.3 × 3.0
WP mass [kg]	5 113	7 975
WP minimum turn radius [m]	0.2	0.4
WP current density [A/mm^2]	153	94
WP inductance [H]	0.14	0.59
WP amp-turns [MA-turns]	10.4	6.3
Terminal current [kA]	40 kA	31.3
Number of turns	256	200
Number of pancakes	16	16
Total REBCO [km]	270	270
Coolant type	Supercritical helium	
Coolant pressure [bar]	10 – 20	15
Operating temperature [K]	20	8 – 17
Peak field on conductor [T]	20.1	23
Peak Lorentz loading [kN/m]	822	750
Magnetic stored energy [MJ]	110	316

the ITER TFMC [12] at a peak field of 8.8 T and the ITER Central Solenoid Model Coil [13] at a peak field of 13 T, the SPARC TFMC achieved over 20-T peak field-on-conductor. Since magnetic stress scales as B^2 and magnetically confined fusion performance scales as B^4, this represents a significant advance in both magnet engineering and fusion device performance. Compared to demonstrated NI magnets [14], which have been primarily built as small-bore nuclear magnet resonance magnets, the TFMC represents a multiple order-of-magnitude increase in engineering parameters such as magnet mass, terminal current, stored magnetic energy, and total superconductor. The objective of this article is to layout the engineering design and implementation that enabled the TFMC to achieve these technical performance metrics.

The rest of this article is organized as follows. Section II covers the requirements and conceptual design. Section III presents the engineering of the major components of the magnet. Section IV provides an overview of the instrumentation package contained within the magnet. Section V discusses major fabrication processes and integration of all components into the final magnet. Finally, Section VI concludes this article with some remarks on the achievements and impact of the TFMC magnet.

II. REQUIREMENTS AND DESIGN OVERVIEW

This section establishes the foundation for the design of the TFMC, providing insight into how the parameters of the SPARC TF magnet influenced the parameters chosen for the TFMC as well as giving an overview of the key high-level technical design and operations concepts that are at the core of the TFMC.

A. Design Requirements

Because TFMC was intended as a risk retirement article for the TF magnet in SPARC, the requirements for the TFMC flowed down from the requirements for the TF, the design of which had to be sufficiently well known at the start of the TFMC Program to satisfy both the plasma physics requirements for the primary confining magnet field of the thermonuclear plasma and the structural and integration requirements within the core of the tokamak complex. In return, key lessons learned from the TFMC have been factored into the design and fabrication of the SPARC TF magnet, which is now underway as of this writing.

A comparison of the final design parameters for the TFMC and one of the eighteen coils from the SPARC TF (as of June 2021) is presented side by side in Table I. It is evident from the table that despite being an approximately 60% scaled version in terms of size and mass and not benefitting from the magnetic field enhancement that comes from being part of a toroidal array, the TFMC achieves well-matched key magnet physics and engineering parameters. These include peak field on conductor, peak Lorentz loading, and magnetic stored energy. Importantly, the TFMC matches these parameters within a similar operational temperature window with sufficiently matched turn-to-turn resistances and inductance to emulate TF-relevant NI magnet dynamics such as charging/discharging and quench evolution.

Achieving such high performance in the subsize single coil, the TFMC required exceeding two important parameters of the TF coil. The first is overdriving the terminal current across the magnet by approximately 30% (40 kA compared with 31.3 kA) in a smaller winding pack (WP). This results in a more aggressive Lorentz loading of the REBCO stacks and potentially more

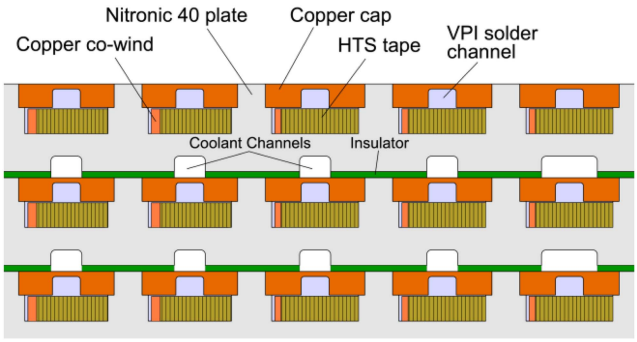

Fig. 2. Partial cross section of the TFMC WP showing the conceptual design of the conductor unit cell.

challenge to the quench resiliency of the coil due to higher WP current density. The second is the tight radii of 20 cm that defines the upper and lower inner corners of the D-shaped magnet. The tight radii were implemented to concentrate magnetic flux and enable exceeding 20-T peak field on conductor. The 20-T peak field on conductor was imposed as a programmatic requirement on the TFMC and used to validate the extrapolation of tape-level to magnet-level performance.

As shown in quench tests and postmortem inspection, the tight radii played a key role in defining a small azimuthal region of the top half of the TFMC WP that sustained burn damage during an intentional open circuit that resulted in a quench. The concentration of magnetic flux in these tight azimuthal regions resulted in well-defined small volumes of suppressed critical current relative to the rest of the WP. As temperature increased in the WP following the open circuit, these regions experienced sustained resistive heating as they transitioned through the critical temperature well in advance of the rest of the WP, ultimately resulting in thermal damage before the rapid quench cascade dissipated the current and stored magnetic energy more uniformly in the magnet. A detailed treatment of the quench dynamics and consequences is presented in [11].

Another important similarity achieved by the TFMC to the TF that is apparent in Table I is the similar mass and size of the magnets. Although 60% smaller, which reduced cost and schedule, the TFMC was intentionally made large enough that the design techniques, principal materials, fabrication processes, and operational aspects of the TFMC could translate directly to the TF. Furthermore, the materials suppliers and fabrication vendors could be identified, proven, and developed as partners not just in the TFMC but also for the TF and the other large-scale magnets required for the SPARC tokamak.

B. Conceptual Design—Thermomechanical

The TFMC and TF designs are based on a grooved stacked plate concept [15] that facilitates the fabrication of mechanically robust high-field superconducting magnets via simple manufacturing techniques from modular components with favorable scaling for commercialization. As shown graphically in Fig. 2, the basic building block is a steel radial plate containing a wound REBCO tape stack and integrated joints embedded within channels; crucially, there is no electrical insulation between turns of the REBCO tape stack. The conductor groove contains a graded stack of REBCO tapes optimized to the magnetic field topology consisting of between 170 and 240 tapes; co-wound copper tapes (henceforth referred to as "copper co-wind") fill the non-REBCO volume in the graded stack and provide additional stabilizer. A copper cap and two copper joint assemblies are located at either end of the REBCO and copper co-wind tape stack. These components are soldered together using a vacuum pressure impregnation (VPI) solder process.

Coolant channels are machined into the other side of the plate. Importantly, the design of the TFMC pancakes enables separating the cooling channel geometry (on one side of the radial plate) from the REBCO stack geometry (on the other side of the radial plate). Coolant flows through the channels from one side of the radial plate to the other, split around the center bore. Thus, rather than spiraling 16 times with the conductor, as it would in a traditional cable-based pancake, the coolant effectively takes only one-half of a turn around the radial plate, which we refer to as "single pass cooling."

A WP is formed by stacking a series of such pancakes together with insulators placed between, except in the region of joint pads, which make pancake-to-pancake (P-to-P) electrical connections. Pancakes and grooves are oriented such that the conductor out-of-plane Lorentz loads are directed toward the bottom of the conductor groove.

A structural coil case surrounding the WP serves as a pressure vessel, both to mechanically constrain the WP and to guide supercritical helium into and out of the pancake coolant channels [16]. This scheme of parallel single-pass coolant channels (two per turn) provides exceptional heat removal from the WP and structural case. It also enables turn-by-turn optimization of the cooling location and capacity throughout the entire WP through the manipulation of the cross-sectional area of the machined cooling channels. These attributes are required in the SPARC TF to remove the large nuclear heat load in the cryogenic superconducting magnets due to the inability to accommodate thick radiation shielding in the compact geometry of the SPARC tokamak.

The radial plates, WP, and the structural case were designed in close coordination to react the Lorentz loading resulting from the combination of azimuthal current and resulting magnetic field. Modeling predicted peak von Mises stresses of approximately 900, 530, and 820 MPa at 40-kA azimuthal current for the individual radial plates, averaged WP, and structural case, respectively. Such loads demanded the use of special steels with high strength at temperatures.

C. Conceptual Design—Electromagnetic

The conductor unit cell geometry, REBCO tape stack size, number of turns, turn-to-turn spacing, and pancake D-shaping was chosen to achieve 20-T peak field on coil with acceptable radial leakage current, acceptable dissipation during charging and discharging, manageable Lorenz loads, and thermally stable

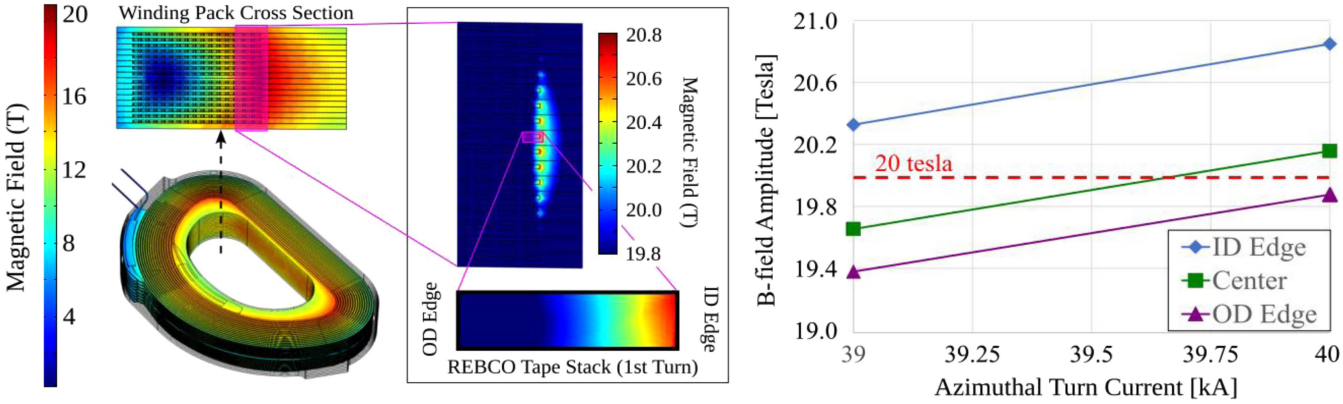

Fig. 3. Predictions for magnetic field in the WP (left) and first turn of Pancake #9 (center). The model predicts that the REBCO tape stack center in the first turn will see approximately 20.1 T at 40 kA, which is the peak field-on-conductor value given in Table I.

operation for all phases. This optimization converged toward a WP that contained 256 turns (16 turns in 16 pancakes) operating at a steady-state current of 40 kA and requiring P-to-P joint resistances of under 5 nΩ. The targeted 20-T peak field on conductor is exceeded in a region around the innermost conductor in the tight bend region of the D-shaped magnet, where the conductor radius of curvature is 200 mm, as shown in Fig. 3. Stored magnetic energy at 40-kA azimuthal turn current is 110 MJ.

D. Electromagnetic Design Verification

An extensive set of electromagnetic (EM) computational tools was developed as a key aspect of the TFMC Program, including lumped element circuit models and coupled 2-D and 3-D finite-element method and Biot–Savart models that accounted for self-fields, magnetic field magnitude and angle-dependent current density distribution, dissipation from joints, and heat removal from coolant. Current distribution within the REBCO stacks is computed self-consistently and not assumed to be uniform. This suite of codes was used to guide the conceptual design of the TFMC in the first part of the project, resulting in the physics foundation around which the magnet engineering was then carried out, and to verify the integrity of the coil fabrication processes during production of the pancakes through interpretation of data obtained during LN2 testing prior to magnet assembly. An example is shown in Fig. 3, where a 3-D electrostatic model is used to predict the peak field on conductor with 40 kA of terminal current in the final design of the TFMC WP. A more complete description of the TFMC code suite and its use throughout the TFMC Program may be found in [11].

III. Engineering Design

The purpose of this section is to provide a technical overview of each of the major components comprising the TFMC, including aspects of design and implementation as well as fabrication details. Details on how each fabricated component was assembled and integrated to form a final magnet are covered in Section V.

A. REBCO Superconductor

Over 300 km of REBCO from multiple manufacters was used as part of the pre-TFMC R&D and the TFMC itself, which utilized over 270 km. Rigorous specifications on superconducting properties, mechanical properties, and geometry were agreed to manufacturers and carefully monitored during the procurement process. The REBCO tape geometry was 4 mm wide with an average thickness of approximately 60 um. Standard REBCO layer composition was used: C276 Hastelloy substrate, buffer layers, REBCO layer, silver coating (∼2 μm) thick), and finally copper stabilizer (∼5 μm per side). After manufacturing, the REBCO was tinned with solder (∼2 μm per side) in a reel-to-reel process at an external vendor to maximize the quality of the VPI solder process described in Section V-B. Measurements of critical current (I_c) were essential. Continuous TAPESTAR™ I_c (77 K, self-field) measurements were taken for every meter of REBCO before solder plating to confirm manufacturer's specification and after solder plating to screen for I_c degradation due to the solder plating process.

The REBCO was then put through an in-house quality assurance and control (QA/QC) process, which combined continuous TAPESTAR™ I_c (self-field, 77 K) measurements of every meter of tape with discrete I_c (B,T,Θ) measurements on statistically selected samples on two platforms: an in-house HTS-110 SuperCurrent ($0 < B < 12$ T, $15 < T < 80$ K, $0 < \Theta < 180°$) [17] and the Tohuku 25T-CSM magnet ($0 < B < 25$ T, $4 < T < 20$ K, $0 < \Theta < 180°$) [18]. The final output of this process provided I_c (B,T,Θ) data for every meter of REBCO in the TFMC. These data were essential for the TFMC Program, providing verification of REBCO performance upon receipt, high-fidelity data for the suite of EM modeling tools for magnet design, and the ability to custom-blend REBCO from the inventory to achieve specific superconducting performance. It should be noted that such detailed understanding of REBCO performance in the TFMC inventory enabled a wide I_c (B,T, Θ) to be accepted from manufacturers, increasing tape yield, lowering cost, and minimizing delivery schedules.

An example output of the REBCO QA/QC process is shown in Fig. 4. The plot contains the engineering critical current density

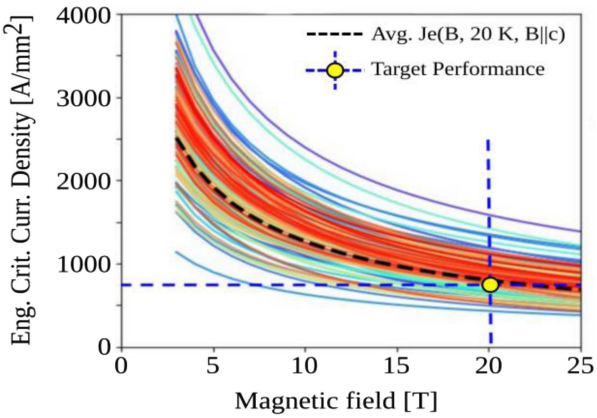

Fig. 4. Example engineering critical current density (J_e) field dependence data for a single shipment of REBCO showing the result of the QA/QC process, in which an average J_e (20 T, 20 K, $B\|c$) prediction can be made for each meter of REBCO received.

(J_e) as a function of magnetic field at 20 K and a field angle of $B\|c$ for one of the many shipments of REBCO received for the TFMC. Despite a wide variation, the average J_e of the shipment (shown by the dotted black line) exceeds the target of 750 A/mm^2 at 20 T, 20 K, and $B\|c$ (shown by the intersection of the dotted blue lines) needed for a single stack of REBCO in the TFMC.

Following the QA/QC process, the REBCO was loaded onto custom reels following a detailed winding plan for each pancake. The winding plan is generated by an in-house winding optimization code using the I_c (B,T,Θ) data generated during the QA/QC process to satisfy the EM requirements of each pancake with an optimized selection of REBCO from the total available inventory. Once the complete set of reels for each pancake was complete, the reels were loaded into an in-house engineered pancake winding machine.

B. Pancakes and Termination Plates

The TFMC contained 16 single pancakes arranged in a vertical assembly and two termination plates, one each at the top and bottom of the stack. Each pancake and termination plate is a complex assembly of components designed to provide the required electrical, mechanical, and thermal properties dictated by the magnet design. There are four different types of pancakes, denoted types A through D. Two types (A and B or C and D) are always adjacent to each other in the stack to ensure that the electrical current, brought from the outer radius to the inner radius by A or C, returns to the outer radius through B or D. Types A and B form one half of the WP; types C and D are simply mirror images of A and B to provide symmetry about the midplane.

The pancakes are composed of four primary subcomponents: 1) the radial plate; 2) the REBCO and copper co-wind stack; 3) inner and outer joint subassemblies; and 4) the copper caps. The radial plates are made from Nitronic 40, which differs from standard 316 stainless steel due to higher manganese and nitrogen content. Nitronic 40 was selected for its high strength and excellent mechanical and fracture properties at cryogenic temperatures (ultimate tensile strength of 1489 MPa and yield strength of 820 MPa at 77 K). While cold-worked steels, such as SS316 LN, can have higher strength, they are unsuited for large radial plate production and the extensive machining required for TFMC-style radial plates. Plates of Nitronic 40 were produced by forging and hot rolled.

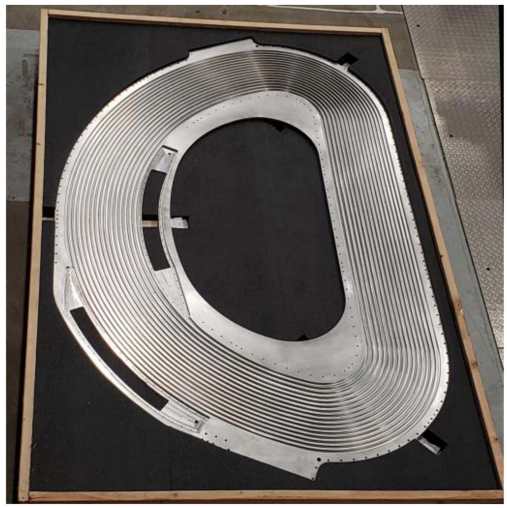

Fig. 5. One of the TFMC radial plates showing the machined channels for the REBCO tape stack and the inner and outer radial pockets for the P-to-P joint subassemblies.

The radial plates were machined on both sides for different purposes: one side received a single spiral channel for the REBCO tape stack with features for the joint subassembly, while the other side received parallel half-turn channels for helium coolant. A view of the REBCO-side of a TFMC radial plate is shown in Fig. 5. The REBCO channel width varied along the winding channel length and is wider at the inner radius and reduces by a few millimeters at the outer radius. The helium channels were machined to optimize coolant flow and thermal management of the pancake according to computational fluid dynamics (CFD). In particular, channels in contact with the inner and outer joints were designed to maximize cooling in these regions where ohmic heating leads to a dominant source of power deposition.

Following machining, the pancakes were transferred to the plating vendor, where uniform nickel coating was applied through an electrocatalytic nickel sulfamate process. The nickel coating is essential for ensuring the REBCO maximizes bonding to the radial plate during the solder process described in detail in Section V.

Once radial plates are complete, REBCO tape stacks of approximately 200 tapes were inserted into the machined channels in a semiautomated winding process. The REBCO tape stacks were terminated at the inner and outer interpancake joint subassemblies. Because the TFMC is composed of single as opposed to the more standard double pancakes, each pancake must have a radially inner and outer joint. Each joint consists of a large copper insert plate, which fitted into a custom detail in the radial plate and is secured by a series of perimeter bolts. The joint also contains hardware to secure the REBCO tape stacks in place under tension for winding as well as space for stainless steel

clamps, which are used to ensure that a joint face compression of 30 MPa is achieved when two pancakes are jointed. The joint plate is sanded, silverplated, and prepared with a mesh of indium wire to maximize the contact surface and minimize electrical resistance.

Once the REBCO tape stacks are in place and terminated securely in the inner and outer joint subassemblies, form-fitting caps are inserted above the REBCO tape stacks to enclose them within the channel. The caps sit on ledges within the machined channel above the REBCO tape stack. The caps were machined from C101 sheets with the same spiral pattern as the radial plates, and, on the bottom surface facing the REBCO, have an internal side-to-side meandering channel machined into them. The channel provides a high-conductance pathway for the molten solder to flow along the 89-m spiral and prevents the tape stack from lifting away from the radial plate due to buoyancy effects in the molten solder and blocking the flow.

The perimeter of the pancake also contains 105 outer diameter (OD) and 82 inner diameter (ID) through holes that enable bolting adjacent pancakes. Bolting of adjacent pancakes alternated between the radially inner and outer perimeters in order to minimize the possibility of axial current transfer between pancakes at regions other than the P-to-P joints. Finally, each pancake was also machined with special holes for steel cylindrical pins to ensure alignment of the interpancake joints during the stacking and assembly process.

The top and bottom termination plates are similar to the pancakes in that machined Nitronic 40 plates with perimeter holes are implemented; however, the termination plates do not contain additional windings but provide two 2-m-long superconducting REBCO terminals, a positive on the bottom and a negative on the top, for electrical current access to the WP. The termination plates also provide the necessary closure for the helium channels for the outermost pancakes.

C. Winding Pack

The core of the WP consists of a stack of 16 pancakes with inner and outer interpancake electrical joints and perimeter mechanical bolts, as shown in Fig. 6. Pancakes were separated from each other with P-to-P insulation. The insulation was made of 1-mm-thick sheets of G-11CR water jet cut into complex shapes that form-fitted the cooling channels of each pancake and allowed the helium cooling to wet the surfaces of the copper caps on the adjacent pancake in the stack. To simplify manufacturing, handling, and assembly, the insulation was designed into individual pieces with interlocking joints at the interfaces. Finally, a top and bottom termination plate complete the stack. The completed WP weighs approximately 5113 kg.

D. Structural Case

The structural case is comprised of three main components: a large bottom Nitronic 50 "trough" weighing 2654 kg, a smaller Nitronic 50 top "cover" weighing 1332 kg, and a thin SS316 LN internal seal plate. At opposite sides of the D-shaped case, the trough and cover pieces are designed with two large 380 by 287 mm openings, or gaps, rimmed with a special bolt pattern

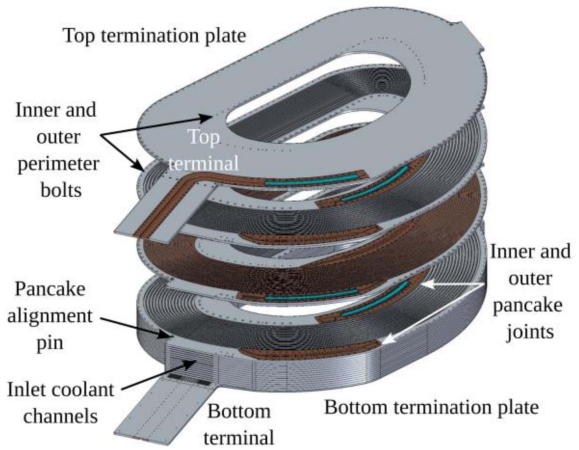

Fig. 6. Rendering of the TFMC WP showing the top termination plate and pancakes #15 and #16 exploded from the 14-pancake stack on the bottom termination plate. The top REBCO terminal that connects to the VIPER feeder system is visible on the top termination plate.

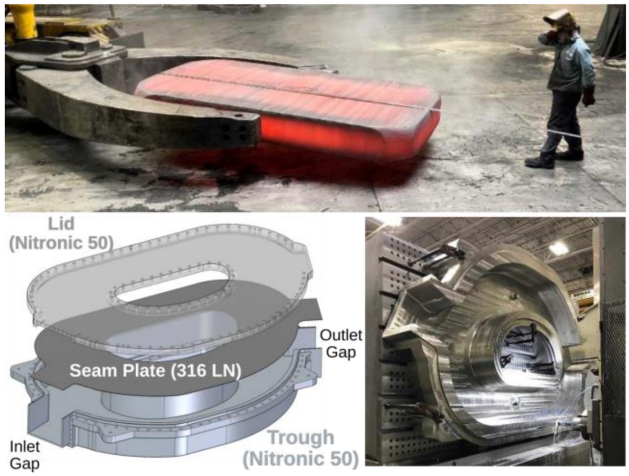

Fig. 7. Final forging for the trough (top), the trough during intermediate inspection checks during machining (bottom right), and an exploded CAD rendering showing how the three pieces of the case (trough, cover, and seam plate) are assembled with gaps for the inlet/outlet plena.

and weld detail to accommodate the installation of pressure vessels, as described in the following subsection. The pressure vessels provide current, helium, and instrumentation access to the WP through the case. The trough and cover pieces are designed to be bolted together with 96 7/8-9 Inconel 718 bolts to provide the structural interface; the SS316 LN internal seal plate, designed to be welded to the trough piece after WP installation, provides the seal between internal high-pressure helium coolant and external high vacuum.

The trough and cover were machined from two large rectangular forgings of Nitronic 50, 18 177 and 6697 kg, respectively; the trough forging is shown after removal from the furnace and during machining in Fig. 7. Machining was chosen over net-shape forging to minimize schedule and because of the unfavorable economics for net-shape forging of a single set of unique objects. Nitronic 50 was chosen for its high mechanical strength at cryogenic temperatures and slightly more favorable welding properties than Nitronic 40. Both slabs were forged and

then air cooled to minimize residual stresses for the later benefit of the machining process. Machining, which was completed to demanding specification proved arduous due to the large volume involved, the strength of the material, and the tight tolerances required to fit the WP. The bottom trough is, to the authors' knowledge, the largest single piece of Nitronic 50 ever machined to a complex final shape.

E. Ground Insulation

Because of the NI nature of the TFMC, the maximum voltage differential in the magnet, which occurs during a quench, was predicted and later confirmed by experiment to not exceed 1 V. Such a low voltage requirement significantly opens up the design space for ground insulation, the primary function of which in the TFMC is to control current paths rather than prevent potentially damaging electrical breakdown. The ground insulation for the TFMC is a hybrid design composed of: 1) stacks of water jet cut G-11CR sheets placed underneath and on top of the WP and 2) epoxy-filled bladders and 5-mil (125-μm) kapton half-lap wrapping on the sides to completely electically insulate and mechanically immobilize the WP within the structural case. The top and bottom stacks of G-11CR sheets were approximately 10 mm in height. The exact stack height was customized to accommodate the as-built height of the WP and provide the designed preload of the WP when the structural case cover is bolted to the trough. The G-11CR sheets included cooling channels to enable helium coolant to flow directly against the case. This results in a simple direct cooling method for the case as well as guaranteeing a minimal temperature gradient between the WP and the case.

To accommodate the WP insertion, the structural case was designed with a 4-mm gap between its inner walls and the outer radial surface of the WP. This gap was filled with custom-sized bladders made from a tough tear-resistant polymer capable of withstanding cryogenic temperatures. Placed empty next to one another to completely fill the radial gap between the WP and the structural case, the bladders were filled in situ during the assembly process with epoxy using peristaltic pumps.

F. High-Pressure Plena (Case Extensions)

To provide an enclosed inlet and outlet for the high-pressure helium coolant as well as access for electrical current and instrumentation wires, two steel case extension pressure vessels, or plena, were attached to openings on either end of the D-shaped structural case. In addition to injecting cold helium, the inlet plenum provided access for the VIPER cables and joint connection to the terminals embedded in the top and bottom termination plates; the outlet plenum provided extraction of the warm helium from the case as well as the instrumentation harnesses from the WP. Both plena are shown and described in Fig. 8. Eight-inch ports were integrated in both plena to provide access to the interior of plena for installation, and two 3-in diameter ports on the outlet plenum served conduits to bring two instrumentation harnesses through the vacuum cryostat port for extraction to the data acquisition system. All components were designed and tested to ASTM pressure vessel boiler code.

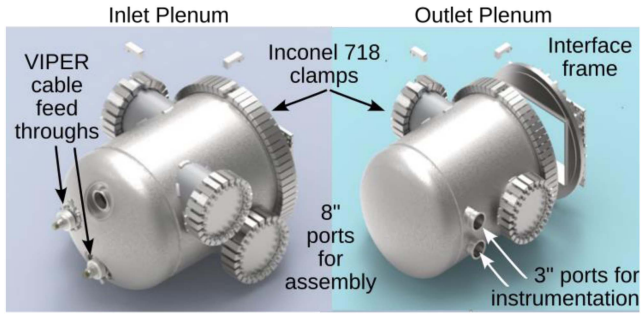

Fig. 8. CAD renderings of the inlet and outlet plena.

The plena were connected to the structural case through an intermediate stainless steel component called the interface frame. For both the plena–frame and frame–case connections, it was desirable to separate the structural load-bearing functionality from the vacuum seal. For the frame–case connection, 32 3/8-16 × 1.5 in (37 mm) long Inconel 718 bolts provided a structural connection to the case, while a weld, with no load bearing requirement, provided the helium-to-vacuum seal. Similarly, for the plena–frame connection, 68 Inconel 718 C-clamps, rather than bolts to accommodate the geometry, provided the structural connection to the plena, while a weld provided the vacuum seal. The advantage of separating these two functions was significant in terms of reducing technical complexity and schedule, enabling the elimination of complex in situ structural welding, potential weld distortations to the plena or structural case, and the need for nondestructive analysis to verify critical structural welds.

G. Current Feedthroughs

One of the challenges introduced by the pressure-vessel style cooling scheme employed was the need to bring up to 45 kA of electrical current across a high differential pressure boundary. The superconducting feeder system, based on VIPER high current REBCO cables [1], sits in vacuum at $\sim 10^{-7}$ torr ($\sim 10^{-5}$ Pa) in the test cryostat. These cables must connect to the TFMC top and bottom termination plate terminals sitting in a 20-bar (2×10^6 Pa) helium atmosphere. To do this, a new high-pressure feedthrough was developed for VIPER cables with a maximum pressure rating of 28 bar at 20 K and a required helium leak rate of less than 10^{-6} torr·L/s. The pressure rating corresponds to the maximum allowable pressure during a magnet quench, when resistive heating of the magnet leads to rapid temperature and pressure rise of the helium in the inlet plena. An in-house R&D program was launched to meet the requirements with standard or easily manufacturable components on an aggressive schedule, as no such commercial component was suitable.

As shown in detail and installed on the inlet plenum in Fig. 9, the successful final feedthroughs (two were fabricated, one for the negative and one for the positive terminal VIPER cables) consisted of a standard NW63 CeFix flange welded to an SS316 high-pressure commercial bellows, which was in turn welded to a machined hollow cylindrical SS316 sleeve. In parallel, the ID of a machined G-11CR sleeve was set with Stycast 2850-FT epoxy to the OD of the prefabricated VIPER cable, which has a

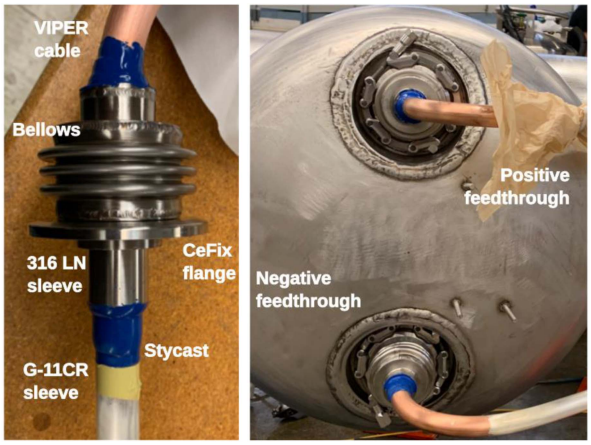

Fig. 9. One of the high-pressure VIPER cable feedthroughs on the benchtop during assembly (left); both feedthroughs and VIPER feeder cables installed on the inlet plenum (right).

solid copper former to maximize conduction cooling. Then, the two subassemblies were joined via the ID of the SS316 sleeve to the OD of the G-11CR sleeve. The entire assembly was then rotated slowly during the entire curing process to ensure highly azimuthal Stycast distribution to eliminate gravity-induced voids in the epoxy layer that would compromise leak tightness. The two feedthrough-cable assemblies were then cycled from room temperature to LN2 rapidly several times followed by a helium leak check qualification test before installation in the plena.

IV. Instrumentation

The purpose of this section is to overview the embedded instrumentation contained within the WP to demonstrate how it was integrated into the engineering design of the magnet as well as to guide the interpretation of experimental results obtained from the TFMC test campaigns [11]. In addition to the information presented here, an extensive array of instrumentation distributed throughout the major subsystems of the TFMC Test Facility provides relevant data for understanding TFMC performance [8].

A. Embedded Instrumentation

The diagnosis of the magnet during operation is essential for achieving the risk retirement objectives of the project for two key reasons. First, it provides experimental validation of the design and fabrication processes as well as the superconducting performance of the magnet; second, it generates data required to validate the extensive multiphysics finite-element analysis models developed in parallel with the TFMC that will be used to design the SPARC TF magnet. As such, a wide array of instrumentation types distributed throughout the WP were required to provide the proper measurements of temperature, voltage, magnetic field, and helium mass flow. Included in the embedded instrumentation package were contact heaters to provide an independent means of probing the coil with energy input to increase local temperatures.

The driving design philosophy for integration of the instrumentation into the WP was to locate all of the instrumentation, including the associated wiring, within the helium coolant channels machined into the backside of the pancake. This had the advantage of maximizing the fraction of the unit cell carrying current to achieve higher engineering current density and protecting all of the instrumentation and wiring during the assembly process. Unlike the REBCO side of the pancake, which is more complex and represents a significant challenge for integration of instrumentation, the helium cooling channels by necessity are completely clear, and instrumentation and wiring represent a negligible obstacle for the helium coolant flow in the channels. One of the consequences of this arrangement is that the voltage taps, both radial turn-to-turn taps and pancake joint-to-joint taps, and Cernox temperature sensors that are installed in the helium channels of a pancake actually measure the voltage of the adjacent pancake by extending through intentional slits cut into the P-to-P G-11CR insulation.

Wiring for all sensors installed in the helium channels is run along the cooling channels and terminated at custom-built printed circuit boards (PCBs) that sit at the exit from each radial plate's cooling channels. These PCBs also contain the turn-to-turn voltage taps, which are spring mounted.

A total 287 individual devices were implemented in the embedded instrumentation of the WP, resulting in approximately 830 signals that had to be extracted from the WP, combined in harnessing, and routed to the helium-atmosphere pressure boundary. Details of the instrumentation devices are as follows.

1) *Voltage taps:* 192 (turn-to-turn) and 19 (joint) differential pairs using pogo pins with steel springs to enable good contact between the tap and the copper cap of the adjacent pancake.
2) *Temperature sensors:* 34 Cernox thin-film RTD sensors were surface mounted to spring-loaded PCBs.
3) *Helium mass flow sensors:* 34 IST model FS2 thin-film flow and directionality sensors were mounted to PCBs at the cooling channel outlets.
4) *Magnetic field Hall effect sensors:* Four cryogenic Hall sensors were bonded directly to the radial plate channel with small corner dots of STYCAST 2850-FT epoxy.
5) *Heaters:* Four "heaterpillars," which are custom-sized arrays of 44 PCB-mounted ruthenium oxide resistors supplied with 16 V in parallel with a total power at 20 K of approximately 50 W.

Of the installed installation, approximately 85% of the voltage taps, 100% of the temperature sensors, 50% of the hall probes, and 50% of the helium flow meters were functional before the final intentional open circuit that concluded the two TFMC test campaigns.

Two views of the instrumentation layout for the WP are presented to convey an understanding of where these critical measurements were acquired. Fig. 10 shows a cross section of both legs of the D-shaped WP: the "curved" outer leg and the "straight" inner leg. The 17×18 (curved leg) and 16×18 (straight leg) matrices represent the grid of machined helium cooling channels formed when the 16 pancakes and two termination plates are stacked and bolted together. Instrumentation

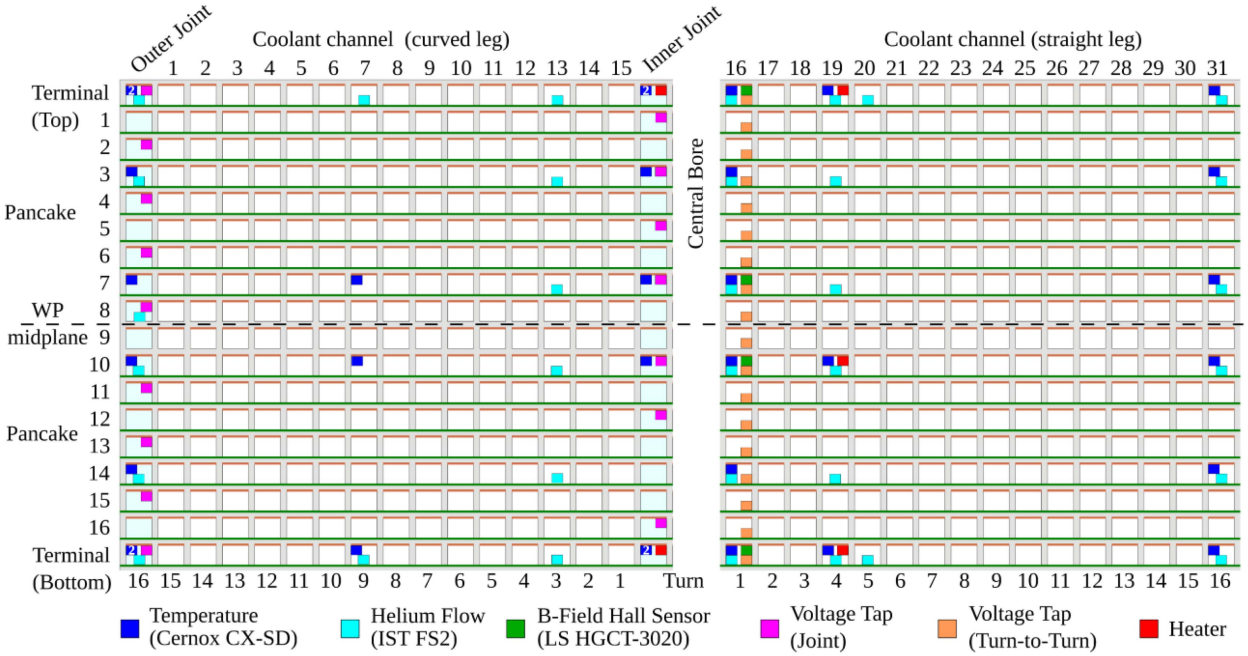

Fig. 10. Cross section of the curved and straight legs of the D-shaped TFMC WP showing the instrumentation map.

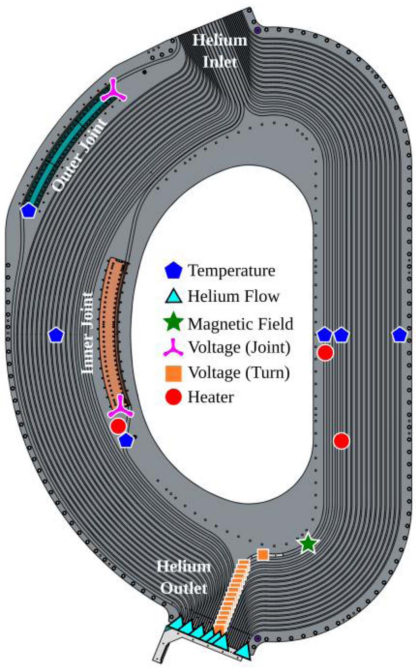

Fig. 11. Plan view of a TFMC pancake showing radial and azimuthal location of the instrumentation.

is indexed by helium channel number at the top of the figure, while corresponding pancake turns are noted at the bottom for reference. Instrumentation occupancy of six types of instrumentation within each channel is denoted by the colored markers. Fig. 11 shows a plan view of a single pancake with the radial and azimuthal location of all instrumentation in corresponding colored markers. Note that this is a collapsed view of all instrumentation to a single view: each pancake only has some subset of these sensors, as seen in the WP cross section of Fig. 10, but they appear in the locations shown here.

Practical limitations on installation time, signal extraction, and data acquisition imposed the need to strategically distribute a finite amount of instrumentation throughout the WP to maximize the science and risk retirement goals of the project. The following strategies are evident from a careful inspection of the instrumentation layout. First, because the P-to-P joints represent the dominant source of heating within the WP in steady-state operation, the joints require careful monitoring to ensure nominal operation. All the joints have voltage taps to provide joint resistance measurements; Cernoxes are present on many of the outer and inner joints, while helium flow sensors ensure that sufficient cooling reaches the resistive joints to remove the ohmic power deposition. Second, because of the complex and novel dynamics expected within the first large-scale NI magnet, particularly during charging/discharging and quench evolution, radial turn-to-turn voltage measurements for most of the 16 turns in all 16 pancakes were considered necessary. The 192 turn-to-turn voltage taps, strategically covering 75% of the turns in the WP, provided the primary window into the superconducting behavior of the TFMC. The total voltage across each pancake was measured separately. Third, because of the innovative pressure-vessel cooling scheme using the machined channels in the radial plate to distribute helium, Cernoxes and helium flow sensors were distributed roughly uniformly throughout the WP to validate the CFD codes used to optimize the helium flow, especially to the joints, and to monitor for potential temperature asymmetries within the WP. Fourth, because the self-generated magnetic field of the TFMC results in minimizing the critical current of the outermost turns, these turns were provided with Cernoxes and helium flow sensors, in addition to the turn-to-turn voltage taps, in order to verify proper cooling

of these regions and to diagnose the onset of current sharing and quench onset as early as possible. Finally, four Hall probes were installed on four pancakes on the innermost turn in the tight inner corner as a secondary measurement system for estimating peak magnetic field on the coil. The primary magnetic field sensors were two three-axis Lake Shore FP Hall probes that were mounted outside of the test facility cryostat and driven by Lake Shore F71 Teslameters. These instruments and their installation are considered part of the TFMC Test Facility and described in detail in [8]; the experimental magnetic field measurements derived from this instrumentation are described in detail in [11].

B. Printed Circuit Boards

Approximately 830 electrical signals from the embedded instrumentation must be extracted from the WP. All the signals, whether they are run on wires from the sensor location through the cooling channel or because the sensors themselves are installed at the channel exit, aggregate just outside the matrix of helium channels, in the open space formed by the gap in the structural case and enclosed by the exit plenum.

The strategy for effectively handling so many signals in a relatively compact space is to borrow from the "card-and-backplane" style of modular electronics crates developed in high-energy physics and other signal-dense application. In this adaptation, 16 custom electronics six-layer PCB instrumentation boards constructed with silver plated FR4 are directly mounted horizontally within the mouth of each pancake and handle the readout of signals from all sensors in each pancake. In addition, the instrumentation boards have a single narrow extension that extends into helium channel 16, radially spanning all 16 turns. All the pogo pin voltage taps used to measure the turn-to-turn voltages in the adjacent pancake are surface mounted to these extensions.

Each of the instrumentation boards connects to a single vertical backplane-style PCB, called the "landing board" that is mounted to the wall of the structural case and aggregates the signals from all sixteen instrumentation boards, as shown in Fig. 12. The landing board distributes a maximum of 1000 signals into ten 100-pin cryogenic compatible connectors (a tenth is provided for future use) for digital packaging into nine discrete wire harness bundles. The harnesses are run through two NW63 flanges on the side of the outlet plenum (see Fig. 8) and then inside stainless-steel instrumentation conduits to high-pressure feedthroughs on one of the radial ports of the main vacuum cryostat, where they pass from the high-pressure helium environment to atmosphere. In order to eliminate potential convection of heat from the warm high-pressure feedthrough back to the 20 K plena through the instrumentation conduits, the conduits were partially filled with expanding spray foam insulation after installation.

V. Final Fabrication and Assembly

This section covers the major fabrication and assembly processes of the TFMC, along with the equipment and tooling produced for those processes, which were required to build the TFMC from its constitutive components.

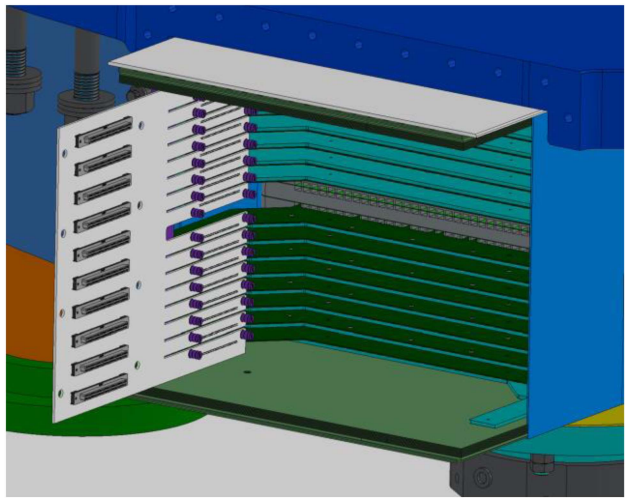

Fig. 12. CAD schematic showing the 16 instrumentation boards mounted to the pancakes at the exits of the helium cooling channels. The vertical landing board is at left.

A. Pancake Assembly

Assembling each of the 16 pancakes and two termination plates is the first step in magnet assembly. First, the surface of the Nitronic-40 radial plate was inspected to ensure that it was within the 1-mm deviation from flatness specification; a clever in-house heat treatment method was developed to correct any out-of-plane deviations due to warping of the radial plate during machining. Second, the radial plate sent to an external vendor for plating. Third, upon return, it is inspected, cleaned with isopropyl alcohol, and installed on the winding table. The REBCO and copper co-wind stack is secured within one of the P-to-P joints, wound into the machined 89-m spiral channel, and secured at the other joint. The pancake's 64 copper caps, split up to minimize schedule via parallel machining and to enable precision tolerances, are inserted into the REBCO channels and rest 0.2 mm above the REBCO stack on small 1-mm ledges machined into the channel. The copper caps must lie flush with the radial plate. Solder paste and wire, as described in the next section, is then applied to fill in the gaps between the sides of the copper caps and REBCO channel walls in the radial plate. At this point, the pancake is ready for installation within a larger compression plate assembly used for the solder process.

B. VPI Solder

Once each pancake has been fully assembled, a VPI solder process is performed. The solder process is adapted and extended from earlier work on solder filling of Nb_3Sn cable-in-conduit conductors [19]. It was initially developed for VIPER cables [20] and then adapted for the NINT-style pancakes in the TFMC [21]. VPI soldering results in a continuous metal matrix in which the REBCO tape stack is fully bonded to the copper caps and the radial plate, as shown in Fig. 13. The result is mechanical stabilization of the REBCO to prevent damage from EM loading during operation, excellent electrical conduction for current

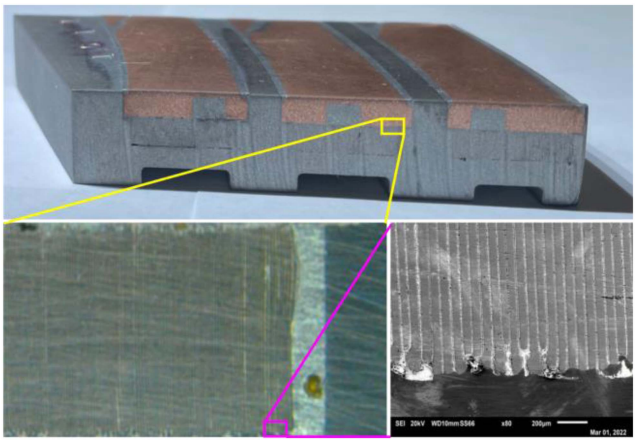

Fig. 13. Cross section acquired during magnet postmortem destructive testing of three turns of a TFMC pancakes (top). A microscope image (bottom-left) and SEM image (bottom-right) shows the high-quality void-free VPI solder that provides mechanical stabilization of the REBCO stack.

Fig. 14. TFMC solder station at MIT showing a pancake VPI solder assembly inside a large convection oven.

sharing and current redistribution, and strong thermal contact to maximize cooling performance [1].

Adaptation of the VPI solder technique to the TFMC from VIPER cables encountered a number of challenges. First, the REBCO channel in the radial plate is an open geometry unlike the VIPER cable, in which the solder flow is completely enclosed within a vacuum-tight cable jacket; a method had to be developed to fully seal the entire pancake and individual channels to provide long-length linear solder flow. Second, the REBCO spiral channel in the radial plate is approximately 89 m long with little void space in the tightly constrained cross section; a method had to be developed to maximize solder flow for long-lengths within the acceptable time–temperature profile required to avoid critical current damage to the REBCO tapes. Finally, a fully assembled TFMC pancake weighs approximately ∼270 kg, which for the VPI solder process translates into a significant thermal load. Methods had to be developed to heat to and cool from the process temperature as rapidly as possible to avoid thermally damaging the REBCO tapes.

In order to meet these and other challenges, several new methods and equipment were developed, many of which can be seen visually in Fig. 14. To enclose the REBCO channel, a set of aluminum plates compresses a gasket, creating a vacuum-tight seal for the intire pancake and between adjacent channels during the solder process. This enables vacuum and pressurized gas to create a monotonic pressure gradient along the channel and ensure a constrained solder flow along the spiral channel. To eliminate deflection of the compression plates under the pressure and temperature cycles, an assembly of large stainless steel ribs was implemented to enhance the stiffness of the aluminum compression plates.

To maximize solder flow, a machined solder channel in the copper cap assured an open flow channel of sufficient hydraulic diameter to enable robust and reproducible flow in a short time. An additional advantage of this channel is to remove the rapid solder flow away from the REBCO tape stack to minimize critical current damage from erosion of the Cu stabilizer layer.

To provide thermal management, the VPI solder process is conducted in a large thermally uniform convection oven. Active heating and cooling systems were implemented within the convection oven to ensure temperature uniformity across the pancake assembly and minimize the time require to bring the assembly up to and down from process temperature to avoid thermal degradation of the critical current. Ninety-six thermocouples distributed throughout the oven, equipment, and compression plate—pancake assembly provided comprehensive monitoring of assembly temperatures.

To fill the space between the sides of the copper caps and the radial plate REBCO channel, which is effectively sealed from the VPI flow channel and is a critical area for mechanical, electrical, and thermal contact provided by the solder, additional solid and paste solder were added on top of the plate in this interstitial space prior to adding the gasket and compression plate. This melted during the thermal cycle, effectively providing reflow solder at the side of the copper caps.

Prior to the solder process, the assembly was leak checked. A fluxing process was then carried out to remove any existing oxides and maximize wetting and solder flow to all components. The solder flow channel was filled with an alcohol-based liquid flux at atmospheric pressure and room temperature. After a 5-min period, the inlet was pressurized to remove as much liquid as possible; however, given the horizontal channel geometry, a significant fraction remained. The assembly was then evacuated, and an extensive Argon purge and backfill process followed to reduce the amount of residual alcohol in the channel.

During the solder VPI process, solder was melted in a large crucible with a siphon to prevent premature flow. The solder and pancake assembly were brought to process temperature under vacuum, and then, pressurized inert gas was applied to the solder. Flow was monitored via a set of contact sensors that detected when solder was present. Additional solder, approximately equal to the amount needed to fill the REBCO channel, was flowed through to an external dump, to ensure good filling and flush out the remaining liquid flux. For later pancake processes, real-time measurements of the dump weight were developed,

which provided useful additional information on flow rate and amount.

The VPI solder process proved to be robust, repeatable, and effective. Each of the 16 pancakes had high solder-filling fraction with few large voids, as shown in the prototypical microscope and scanning electron microscopic (SEM) images of the RE-BCO tape stacks of Fig. 13. Small voids were observed during the postmortem computer tomography imaging and destructive testing in a few locations. The cause is attributed to two effects. First, incomplete flushing of the flux, particularly underneath the tape stack or copper cap, results in contamination that prevents proper solder wetting and bonding of components. Second, solder shrinkage (approximately 4% by volume) during cooldown, mainly in the flow channel, can lead to small improperly filled areas. Where present, these small voids, in principle, may have resulted in damage to a few unsupported REBCO tapes in these areas due to expansion and strain under high EM loading. While some evidence of this was captured in postmortem micrographs of REBCO near voids, such damage was highly localized and affected only a few tapes out of an approximately 200-tape stack; no critical current degradation attributable to this effect was measured during extensive testing of the TFMC [11].

Overall, the solder process was optimized to avoid critical current damage to REBCO tapes with a target of sustaining no more than 5% critical current degradation (as measured at 77 K during pancake qualification tests) from all assembly- and solder-based processes. Thermal uniformity across the pancake assembly of ± 1 °C at process temperature was achieved during the solder flow process. The assembly was uniformly brought to temperature in approximately 4.5 h with an average solder flow time in the range of 10–15 min. The process time–temperature profile, as well as active heating before and cooling after the solder flow completed, was implemented to limit thermal degradation of REBCO. After soldering, pancakes were removed from the compression plates and cleaned to remove excess solder and residual debris.

Following soldering, each pancake was electrically tested in LN2 to quantify critical current degradation sustained by the pancake winding, assembly, and soldering process. Comparisons between predictive models and experimental results showed that all pancakes experienced an acceptable 1.5–4.0% total degradation of critical current, as shown in Fig. 15. Multiple short pieces of REBCO witness samples attached to the radial plates at different points within the compression plate assembly during the solder cycle showed a similar 0.1–3.0% critical current degradation, corroborating the pancake measurements.

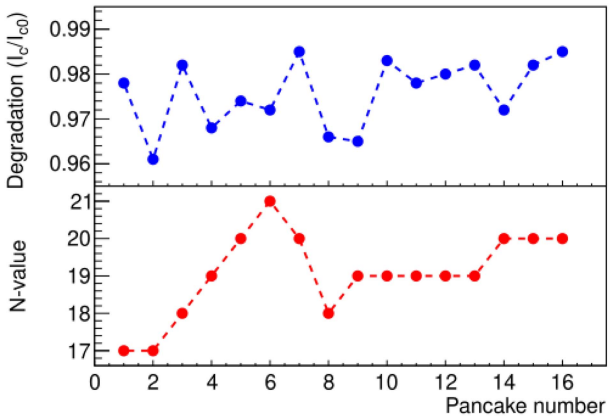

Fig. 15. Results of postsolder LN2 testing showing minimal critical degradation and good n-value for all 16 pancakes.

TABLE II
STACKING SEQUENCE FOR THE TFMC WP

Order	Pancake
17	Top Termination Plate
16	D4
15	C4
14	D2
13	C3
12	D3
11	C2
10	D1
9	C1
8	B3
7	A3
6	B2
5	A1
4	B1
3	A2
2	B5
1	A4
0	Bottom Termination Plate

C. Magnet Assembly

The TFMC was designed to be assembled in the following order. First, the 16 pancakes and two termination plates were stacked and bolted to form the WP; then, the WP was inserted into the structure case; finally, the plena, instrumentation boards, and current lead connections were made to complete the magnet.

As described in detail in Section II, four pancakes of each of the four different configurations (A, B, C, and D) were stacked in a specific configuration to make the WP. The stacking order of the pancakes in shown in Table II. All pancakes were completed and tested in LN2 in order to provide an optimized stacking order that maximized the performance of the TFMC based on the as-built performance of each individual pancake.

Stacking was performed on a custom-designed tool composed of a thick aluminum plate supported by eight jack screws for precise leveling and stiffness while allowing ample access to the ID and OD of the pancakes for ease of stacking. All connections and processes during assembly were designed to be accessible from the top surface of the pancakes including: the installation of the P-to-P perimeter bolts; the assembly of the joint clamps; installation of the P-to-P G-11CR insulation; and the insertion of two pancake alignment pins. The stacking process required the bolting of the P-to-P perimeter bolts (OD-A&C type and ID-B&D type), the torquing of the joint clamps to the previeous

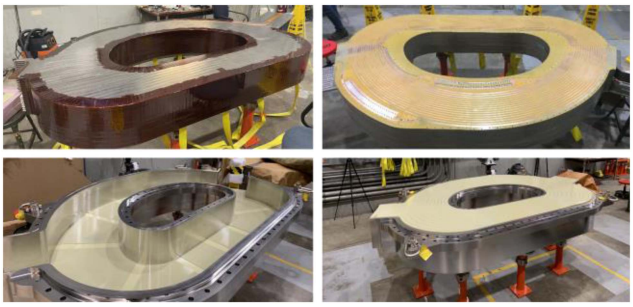

Fig. 16. WP with half-lap Kapton (top-left) and with G-11CR sheet ground insulation (top-right). The structural case with G-11CR sheet ground insulation before (bottom-left) and after (bottom right) insertion of the finding pack.

pancake, the installation of the P-to-P insulation, and application of the indium wire at the joint interface for the next pancake. All A&B-type pancakes were stacked with the copper caps facing vertically down (cooling grooves vertically up). At the midplane of the WP, the pancake types change to C&D (mirror images of A&B type). C&D pancakes are stacked with the copper caps faced upward. This process ensures that the TFMC EM centering load acting on the HTS conductor pressed against the radial plate. With every stacked pancake, its respective instruments were installed and checked, before and after stacking of the pancake. While not intentionally part of the instrumentation design, the electrical connectivity check provided by the pogo pin voltage taps on the most recently installed pancake connecting with the adjacent pancake provided an intrinsic sensitive diagnostic of P-to-P flatness during the stacking process. This proved invaluable in identifying and eliminating physical gaps in some of the P-to-P electrical joints.

In preparation for the insertion of the WP into the structural case, the ground insulation was applied, as shown in Fig. 16. The ground insulation is a hybrid design composed of G-11CR sheets 1–2 mm thick placed between the bottom and top of the WP and the structural case. This stack of insulation plates was approximately 10 mm thick. A half-lap kapton wrap (0.005 in thick with adhesive) was applied on the ID and OD perimeter walls. The top and bottom insulation sheets were used to center the WP inside the case as well as for tolerance buildup adjustments.

For the insertion of the WP into the trough, a chandelier-style spreader tool was used, as shown in Fig. 17. A total of ten polyester rigging straps cradle the WP; the straps are attached to a series of turnbuckles and rigging wires, which enabled precision leveling and even distribution of the load while providing a large safety factor. A 10-t overhead crane guided the chandelier-style spreader over the case trough, where a series of alignment guides fixed to the top surface of the trough helped guide the precise insertion of the WP into the trough. The trapped polyester straps were cut at one end and pulled out through precut grooves in the G-11CR insulation.

The 4-mm gap between the WP and the case was filled, as discribed in Section III-E. The entire process took less than one day and proceeded without incident. The epoxy was allowed to cure overnight, at which time the excess bladder material above

Fig. 17. Winding being installed into the structural case using the chandelier-style spreader assembly.

Fig. 18. Following installation of the WP, the structural case cover is bolted to the trough.

the WP was cut off the next morning. The epoxy system fully cured within a 48-h period.

The next step was the installation of the top G-11CR ground insulation sheets to fill the space between the top of the WP and the top of the case. At this point, the top ground insulation total height was adjusted to compensate for WP stack tolerances. The SS316 LN seam plate was welded to the top surface of the structural case trough. Prior to the installation of the structural case cover, the seam plate was helium leak checked. The cover was then bolted to the trough by 96 7/8–9 UNC Inconel 718 bolts, as shown in Fig. 18.

The final step in the assembly of the TFMC was the installation of the two plena, including the VIPER feeder cables at the inlet plenum and instrumentation harnessing at the oulet plenum. These two components were attached to either end of the D shape TFMC case via an interface frame. The interface t5frame is bolted by 32 Inconel 718 bolts and seam welded to the TFMC case openings. In this design, the bolts carried the EM and pressure loads, while the weld provided the vacuum seal. This same concept was used to secure the plena to the interface frame. A series of 86 Inconel 718 custom-designed clamps secured the plena to the interface frame and carried the pressure and EM loads, while a perimeter weld provided the vacuum seal.

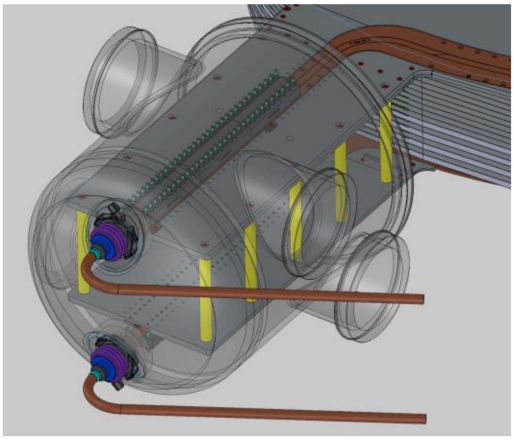

Fig. 19. CAD rendering of the inlet plenum installed on the TFMC. The VIPER feeder cables with high-pressure feedthroughs are visible in the foreground, while the joint between the feeder cables and the top TFMC termination plate terminal is visible inside the transparent plenum.

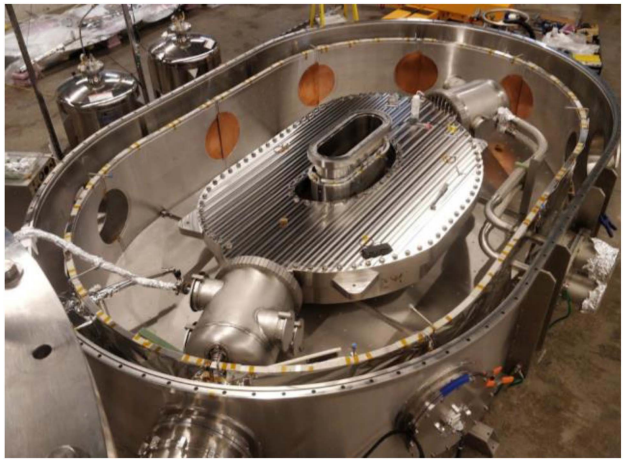

Fig. 20. TFMC being prepared for testing within the vacuum cryostat of the TFMC test facility at MIT PSFC.

The two VIPER feeder cables prebonded to the high-pressure feedthroughs were then installed onto NW63 CeFex flanges on the inlet plena, as shown in Fig. 9. The feeder cables each connect to the superconducting terminals of the top and bottom termination plates with a 400-mm-long joint, as shown in Fig. 19.

Approximately 830 instrumentation wires, carrying signals from the embedded instrumentation within the WP, were bundled together and routed through two NW63 flanges on the outlet plenum and through the high-pressure steel conduit that would connect to an external flange of the test facility. The harnesses were secured in place in readiness for magnet installation. Access to the wire and connection was provided by three 8-in ports on the side of the outlet plenum.

At this point, the assembly process was considered finished, and the TFMC was a complete magnet ready for testing. As described in more detail in companion papers within this special issue, the TFMC was successfully rigged and installed into the large vacuum cryostat at the heart of the TFMC test facility, with connections made between the facility and the TFMC to provide electrical current, helium coolant, and instrumentation extraction, as shown in Fig. 20 [8]. After successfully passing room temperature checks followed by vacuum pumpdown and cooldown to 20 K, the TFMC was sucessfully tested to over 20-T peak field on conductor in September 2021 followed by a series of more extensive thermal scans and quench tests in October and November of 2021 [11].

VI. Conclusion

This article presented the design, fabrication, and assembly of the SPARC TFMC, the first large-scale high-field REBCO superconducting magnet built. Building on a decade of R&D on NI REBCO magnet technology at MIT starting in 2010 [22], the TFMC transformed small-bore REBCO NI technology into large-scale fusion-scale REBCO magnets. It did this in two ways: first, by adapting the simple design and less complex fabrication techniques of small-bore NI magnets to large-scale fusion-style superconducting magnets and, second, by introducing several new innovations including the REBCO stack-in-plate unit cell, the cryogenic pressure-vessel style cooling approach, and robust low-resistance demountable P-to-P joints. As presented in this special issue's paper on experimental results [11], the TFMC was used in two experimental test campaigns in the Fall of 2021. In September 2021, the TFMC successfully achieving all its dc test objectives including exceeding 20-T peak field on conductor. In October 2021, it then underwent a series of temperature scans and open-circuit quenches to provide extensive data on current sharing and quench evolution for physics understanding and model validation. The performance of the magnet during the test campaigns, as well as detailed postmortem destructive and nondestructive testing of the coil after testing, confirmed that the engineering design, component fabrication, and magnet assembly were executed exactly as intended to implement the physics design of the coil within challenging specifications.

Following the success of the TFMC Program, superconducting magnet R&D at CFS and MIT has leveraged the technological advances, lessons learned, and fabrication and test facilities on two paths: first, the continued development of large-scale high-field quench-resilient steady-state NI magnets for the SPARC TF magnet and, second, the adaptation of the VIPER cable for low ac losses to serve in the pulsed SPARC central solenoid and poloidal field coils. Similarly, outside of the SPARC Project, the REBCO magnet technology and capabilities from the TFMC Project are being deployed in other superconducting magnet systems for fusion energy and high-energy physics, including the first nonplanar REBCO stellarator coil based on VIPER cable [23]. The authors hope that the success of the TFMC Project and those that follow inspire and enable new advances in superconducting magnet technology for the entire community and open new possibilities for high-field magnet science and applications.

ACKNOWLEDGMENT

The parties have pursued patent protection relating to inventions. CFS has exclusive commercial rights to the technology for energy generation. The magnet technology in the TFMC Program was developed under research collaborations between the Massachusetts Institute of Technology and CFS. The authors would like to thank the entire TFMC Project team from MIT and CFS. The authors would also like to thank the following vendor partners, who delivered challenging pieces on aggressive schedules while working at risk through the difficulties of the COVID-19 pandemic. This project would not have been possible without their commitment: ACP Waterjet, Dav-Tech Plating, Electralloy, Gilchrist Machine, G. O. Carlson, HTS-110, Incodema, Luvata, Paragon D&E, Reno Machine, Scott Forge, Toupin Rigging, and Wisconsin Oven Corporation. The authors would also like to personally thank the following individuals: Prof. Ron Ballinger of MIT for rather timely advice on metallurgy and forgings; Corinne Cotta and Tesha Myers from MIT PSFC for outstanding leadership on procurement and fiscal support, respectively; Andrea Jarrett and Joseph Stiebler from CFS for procurement support; and Jeff Mullins of Oliver Welding for expert in situ vacuum and high-pressure welding.

REFERENCES

[1] Z. S. Hartwig et al., "VIPER: An industrially scalable high-current high-temperature superconductor cable," *Supercond. Sci. Technol.*, vol. 33, no. 11, Oct. 2020, Art. no. 11LT01, doi: 10.1088/1361-6668/abb8c0.

[2] E. E. Salazar et al., "Fiber optic quench detection for large-scale HTS magnets demonstrated on VIPER cable during high-fidelity testing at the SULTAN facility," *Supercond. Sci. Technol.*, vol. 34, no. 3, Feb. 2021, Art. no. 035027, doi: 10.1088/1361-6668/abdba8.

[3] V. Fry, J. Estrada, P. C. Michael, E. E. Salazar, R. F. Vieira, and Z. S. Hartwig, "Simultaneous transverse loading and axial strain for REBCO cable tests in the SULTAN facility," *Supercond. Sci. Technol.*, vol. 35, no. 7, May 2022, Art. no. 075007, doi: 10.1088/1361-6668/ac6bcc.

[4] B. Labombard et al., "Spiral-grooved, stacked-plate superconducting magnets and related construction techniques," U.S. Patent US20 200 211 744A1, Jul. 2, 2020.

[5] D. Whyte, "Small, modular and economically attractive fusion enabled by high temperature superconductors," *Philos. Trans. Roy. Soc. A: Math., Phys. Eng. Sci.*, vol. 377, no. 2141, Mar. 2019, Art. no. 20180354, doi: 10.1098/rsta.2018.0354.

[6] A. J. Creely et al., "Overview of the SPARC tokamak," *J. Plasma Phys.*, vol. 86, no. 5, Oct. 2020, doi: 10.1017/S0022377820001257.

[7] Z. Hartwig et al., "The SPARC Toroidal Field Model Coil Program," *IEEE Trans. Appl. Supercond.*, vol. 34, no. 2, Mar. 2024, Art. no. 0600316.

[8] T. Golfinopoulos, "The SPARC Toroidal Field Model Coil Magnet test facility," no. Special Issue on the SPARC Toroidal Field Model Coil, 2023.

[9] V. Fry et al., "50 kA capacity, nitrogen-cooled, demountable current leads for the SPARC toroidal field model coil," *IEEE Trans. Appl. Supercond.*, early access, Jan. 16, 2024, doi: 10.1109/TASC.2024.3354237.

[10] P. C. Michael et al., "A 20 K, 600 W, cryocooler-based supercritical helium system for the SPARC toroidal field model coil," *IEEE Trans. Appl. Supercond.*, vol. 34, no. 2, Mar. 2024, Art. no. 0600113.

[11] D. G. Whyte et al., "Experimental results from the SPARC toroidal field model coil test campaigns," *IEEE Trans. Appl. Supercond.*, vol. 34, no. 2, Mar. 2024, Art. no. 0600218, doi: 10.1109/TASC.2023.3332823.

[12] A. Ulbricht et al., "The ITER Toroidal Field Model Coil Project," *Fusion Eng. Des.*, vol. 73, no. 2, pp. 189–327, Oct. 2005, doi: 10.1016/j.fusengdes.2005.07.002.

[13] R. J. Jayakumar, J. V. Minervini, J. Wohlwend, N. Martovetsky, and R. J. Thome, "The USHT-ITER CS model coil program achievements," *IEEE Trans. Appl. Supercond.*, vol. 10, no. 1, pp. 560–563, Mar. 2000, doi: 10.1109/77.828296.

[14] S. Hahn et al., "45.5-tesla direct-current magnetic field generated with a high-temperature superconducting magnet," *Nature*, vol. 570, Jun. 2019, Art. no. 7762, doi: 10.1038/s41586-019-1293-1.

[15] B. Labombard et al., "Grooved, stacked-plate superconducting magnets and electrically conductive terminal blocks and related construction techniques," U.S. Patent US11 417 464B2, Aug. 16, 2022.

[16] B. Labombard, R. Mumgaard, W. Beck, and J. Doody, "Conductor and coolant schemes for spiral-grooved, stacked plate, non-insulated superconducting magnets," Patent CA3167302A1, Sep. 30, 2021.

[17] N. M. Strickland et al., "Extended-performance 'supercurrent' cryogen-free transport critical-current measurement system," *IEEE Trans. Appl. Supercond.*, vol. 31, no. 5, Aug. 2021, Art. no. 9000305, doi: 10.1109/TASC.2021.3060355.

[18] S. Awaji et al., "First performance test of a 25 T cryogen-free superconducting magnet," *Supercond. Sci. Technol.*, vol. 30, no. 6, May 2017, Art. no. 065001, doi: 10.1088/1361-6668/aa6676.

[19] P. Bauer et al., "Solder-filling of a CICC cable for the EFDA Dipole Magnet," *AIP Conf. Proc.*, vol. 986, no. 1, pp. 151–158, Mar. 2008, doi: 10.1063/1.2900339.

[20] A. Hubbard, "Processes, systems and devices for metal filling of high temperature superconductor cables," U.S. Patent PCT/US2020/060170, May 20, 2021.

[21] A. Hubbard, "Processes, systems and devices for metal-filling of open HTS channels," U.S. Patent 63/279 443, 2022.

[22] S. Hahn, D. K. Park, J. Bascunan, and Y. Iwasa, "HTS pancake coils without turn-to-turn insulation," *IEEE Trans. Appl. Supercond.*, vol. 21, no. 3, pp. 1592–1595, Jun. 2011, doi: 10.1109/TASC.2010.2093492.

[23] N. Riva, "Development of the first multi-turn non-planar REBCO stellarator coil using VIPER cable," *Supercond. Sci. Technol.*, vol. 36, 2023, Art. no. 105001, doi: 10.1088/1361-6668/aced9d.